

Impacts of Sample Size on Calculation of Pavement Texture Indicators with 1mm 3D Surface Data

46(1), pp. 42-49, 2018

<https://doi.org/10.3311/PPtr.9587>

Creative Commons Attribution 

Lin Li^{1*}, Kelvin C.P. Wang², Qiang Li², Wenting Luo¹, Jiangang Guo¹

RESEARCH ARTICLE

Received 12 June 2016; accepted 19 December 2016

Abstract

The emerging 1mm resolution 3D data collection technology is capable of covering the entire pavement surface, and provides more data sets than traditional line-of-sight data collection systems. As a result, quantifying the impact of sample size including sample width and sample length on the calculation of pavement texture indicators is becoming possible. In this study, 1mm 3D texture data are collected and processed at seven test sites using the PaveVision3D Ultra system. Analysis of Variance (ANOVA) test and linear regression models are developed to investigate various sample length and width on the calculation of three widely used texture indicators: Mean Profile Depth (MPD), Mean Texture Depth (MTD) and Power Spectra Density (PSD). Since the current ASTM standards and other procedures cannot be directly applied to 3D surface for production due to a lack of definitions, the results from this research are beneficial in the process to standardize texture indicators' computations with 1mm 3D surface data of pavements.

Keywords

pavement texture indicators, Mean Texture Depth (MTD), Mean Profile Depth (MPD), Power Spectral Density (PSD), pass filter, 3D Data

1 Introduction

The primary function of a pavement is to provide safety and smoothness for the traveling public. Several studies indicate that these functional characteristics are highly associated with pavement texture properties (Ergun and Agar, 2010; Flintsch et al., Li and Wang, 2016; Torbruegge and Wies, 2015; Meegoda and Gao, 2015). Pavement surface texture is defined as the deviation of the pavement surface from a true planar surface or an ideal shape (ASTM E867, 2012). These deviations occur at several distinct levels of scale, each defined by wavelength (λ) (Hall et al., 2006), such as micro-texture ($\lambda < 0.5\text{mm}$), macro-texture ($0.5 < \lambda < 50\text{mm}$), mega-texture ($50 < \lambda < 500\text{mm}$), and roughness or unevenness ($\lambda > 500\text{mm}$) (ISO Standard 13473; 1997; Sengoz et al., 2012).

It is widely recognized that pavement surface texture influences pavement–tire interactions. Skid resistance on a road surface is affected by both micro-texture and macro-texture (Li and Wang, 2016; Torbruegge and Wies, 2015; Meegoda and Gao, 2015; Hall et al., 2006), and wet pavement friction is primarily affected by macro-texture (Ergun and Agar, 2010; Luo et al., 2014). In the past decades, several indicators have been proposed and used to characterize the pavement surface texture, such as Mean Profile Depth (MPD), Mean Texture Depth (MTD), Hessian Model, and Power Spectral Density (PSD) (Wang et al., 2012; Abbas et al., ASTM E2157-15, 2015; ASTM E1845-15, 2015; ASTM E965-15, 2015; Luo et al., 2016; Gendy and Shalaby, 2007; Sayers and Karamihas, 1996; ASME B46.1, 2009). However, these research efforts did not address the impact of sample size (sample length and width) on the calculation of these indicators since the traditional data collection systems were used in the past practices.

The objective of this paper is to investigate the impacts of sample widths and lengths on the computation of texture indicators using data collected from the emerging 1mm resolution 3D data collection technology. The following tasks are conducted: (1) to extract the height or depth values and repair invalid readings from the 1mm 3D raw data; (2) to utilize image processing techniques to eliminate unwanted wavelengths; (3) to calculate texture indicators in spatial domain (e.g. MPD and MTD) and

¹ College of Transportation and Civil Engineering, Fujian Agriculture and Forestry University, Fuzhou, Fujian Province, 350002, China

² School of Civil and Environmental Engineering, Oklahoma State University, Stillwater Ok, USA 74078, USA

* Corresponding author, e-mail: lilin531@gmail.com

in frequency domain (e.g. PSD), at various sample lengths or widths; and (4) to investigate the impacts of sample size on the calculation of these texture indicators based on Analysis of Variance (ANOVA) test and linear regression methods.

2 Texture Data Acquisition System

2.1 Digital Highway Data Vehicle (DHDV)

DHDV, developed by the WayLink Systems Corporation with collaborations from the University of Arkansas and the Oklahoma State University, has been evolved into the sophisticated system to conduct full lane 2D/3D data collection on roadways at highway speed up to 100 km/h with the PavVision3D sensors. DHDV is a real-time multi-functional system for roadway data acquisition and analysis, particularly for pavement surface distress survey, roughness- and safety-related pavement performance evaluation (Wang et al., 2008).

With the latest PavVision3D Ultra (3D Ultra in short), the resolution of surface texture data in vertical direction is about 0.3 mm and in the longitudinal direction is approximately 1 mm at 100 km/h data collection speed. Fig. 1 (a) shows the exterior appearance. Fig. 1 (b) shows rear view of the DHDV equipped with the 3D Ultra technology. With the high power line laser projection system and custom optic filters, DHDV can work at highway speed during day-time and night-time and maintain image quality and consistency. 3D Ultra is the latest imaging sensor technology that is able to acquire both 2D and 3D laser imaging data from pavement surface through two separate left and right sensors. The camera and laser working principle is shown in Fig. 1 (c). By illuminating a surface using a line laser and shooting 3D images using the 3D cameras, the surface variation in the vertical direction can be captured with the triangulation principle that determines the distance from the camera to the pavement based on the laser point (e.g. P1 or P2). Examples of 3D pavement surface image with detailed features are illustrated in Fig. 2.



Fig. 1 Photographs of (a) DHDV exterior appearance (b) DHDV rear view with PavVision3D sensors; (c) Pavvision3D working principle

2.2 Test Sites

Seven pavement sites located in Fayetteville Arkansas are tested to investigate the impacts of sample size on the computation of texture indicators in this study. Three PCC pavements and four AC pavements are included. For each test site, the section length, GPS coordinates, the number of 1mm raw 3D images collected, surface type and pavement condition rating are described in Table 1.

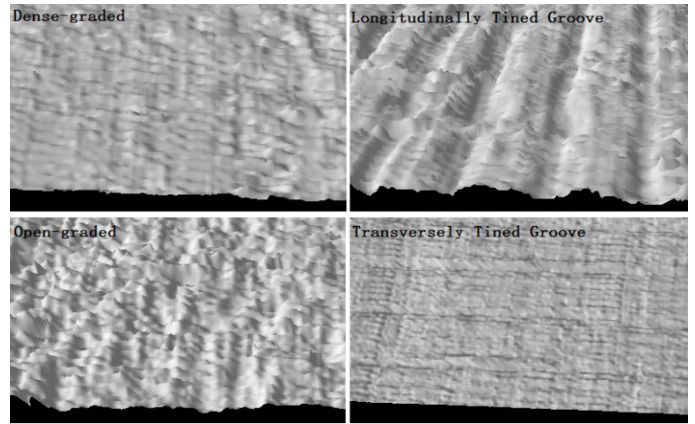


Fig. 2 Examples of 1mm 3D pavement surface image with texture details.

Table 1 Summary of seven test sites for AC and PCC pavements

ID	Surface Type	Length (m)	Condition	# of Images
1	AC (Dense-graded)	643.74	Fair	1139
2	AC (Dense-graded)	611.55	Poor	1072
3	AC (Open-graded)	547.18	Good	956
4	AC (Dense-graded)	514.99	Good	897
5	PCC (Burlap dragged)	225.31	Fair	85
6	PCC (Tined texture)	241.40	Fair	38
7	PCC (Tined texture)	257.49	Poor	58

3 Surface Texture Indicators

3.1 Mean Profile Depth (MPD)

MPD is a widely accepted and used texture indicator. It is defined as the average of all mean segment depths of all segments of the profile. The computation of MPD is described as follows (ASTM E1845-15, 2015): 1) the measured profile is divided into different segments having a length of 100 ± 2 mm; 2) the segment is divided into two equal halves and the height of the highest peak in each half segment is determined; 3) the average of these two peak heights minus the average of all heights is the Mean Segment Depth (MSD); 4) the average value of the mean segment depths for all segments making up the measured profile is reported as the MPD, as shown in Fig. 3.

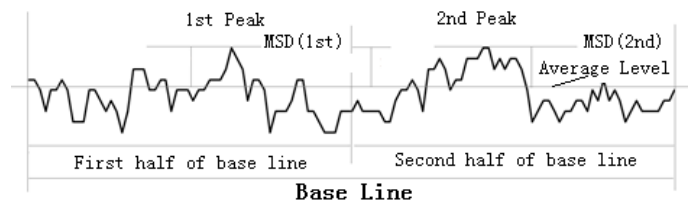


Fig. 3 A general procedure for MPD Calculation

3.2 Mean Texture Depth (SMTD)

MTD represents a 3D surface characteristic since it is obtained by simulating volumetric measuring technique such as the sand path method (ASTM E965-15, 2015). Typically, MTD can be either measured in the field or converted from MPD under 2D environments.

In this paper, the MTD computation is based on 3D texture image with 1mm resolution. Assuming each sample is divided into K small grids and each grid has a size of $N \times M$ mm, the MTD of the entire sample is the average of the MTDs computed at each grid, as described in (1)

$$MTD = \frac{1}{K} \times \sum_{i=1}^K \frac{\sum_{x=1}^N \sum_{y=1}^M [F_0 - F(x, y)]}{D}. \quad (1)$$

Where: $F(x, y)$ - the pixel depth at point (x, y) , D - the integral or gridded area consisting of $M \times N$ pixels, F_0 - the maximum peak in each area D ; K - the number of grids within the test sample.

3.3 Power Spectra Density (PSD)

PSD is a statistical representation of the importance of various wave numbers in the frequency domain (Sayers and Karamihas, 1996). Typically two methods are widely used to compute PSD for road profiles: one based on autocorrelation function; the other based on Fourier Transform (Abbas et al., 2007). In this research the second method is used. Typically, Fourier Transform can be mathematically expressed as (2).

$$F(k, l) = \sum_{i=0}^{N-1} \sum_{j=0}^{M-1} f(m, n) e^{-i2\pi \left(\frac{km}{N} + \frac{ln}{M} \right)}. \quad (2)$$

Where N and M represent the image size, $f(m, n)$ is the intensity value at pixel (m, n) ; $F(k, l)$ is the transformed amplitude at frequency (k, l) or wave number (k, l) .

PSD amplitude at each single frequency can be computed by (3), and the average of the sum of amplitudes over different frequencies is used to represent the averaged PSD in the sample.

$$PSD(j, k) = |Re(j, k)|^2 + |Im(j, k)|^2. \quad (3)$$

Where j and k represent the coordinates of wave number in Fourier image, the $Re(j, k)$ represents the real part of a complex variable in u and v directions in frequency domain, and the $Im(j, k)$ represents the imaginary part of this complex.

4 Data Pre-Processing

4.1 Sample Preparation

Currently there is no consensus on the wheel path locations for surface texture characterization (Sayers and Karamihas, 1996). It should be noted that pavement surface texture of interest is primarily concentrated at the contact areas between pavement surface and vehicle tires. In this paper the contact area with a width of 256 mm is used as the wheel-path to perform texture analysis.

The size of each image is approximately 2048mm in width by 512mm in length. The 1mm 3D raw images are used as the basic elements to constitute a sample. Afterwards, data processing

and analysis is conducted on each sample. To investigate the effects of sample size on the calculation of texture indicators, five different sample lengths and five different sample widths are examined. At each test site, the calculation of each texture indicator is based on various sample lengths or widths, as illustrated in Table 2.

Table 2 Sample lengths and widths for the calculation of texture indicators

Test ID	# of raw images	Sample lengths (m)	Sample widths (mm)				
			256	64	16	4	1
1	1	0.5	×				
2	2	1	×				
3	4	2	×		Not included		
4	8	4	×				
5	16	8	×	×	×	×	×

4.2 Invalid Data Repair

Due to illumination unevenness and noise in laser optics, there are small percentages of 3D data points that have unusually high values or zero values. These invalid pixels or readings are not actual representations of the pavement surface texture; thereby they should be repaired with image processing techniques.

In this study the neighbourhood averaging method is used. This method generally includes (1) a neighbourhood centered at the invalid reading, and (2) a predefined mask with identical or distinct weight values for each pixel. A new pixel value with coordinates is obtained by convolving the predefined weight mask with the neighbourhood centered at the invalid reading. Afterwards, the invalid reading is repaired by replacing it with the new obtained pixel value.

For instance, at any invalid point, $f(x, y)$, in the image, the response, $g(x, y)$, is the sum of products of the mask coefficients, $w(s, t)$, and their corresponding neighbourhood image pixels, $f(x + s, y + t)$, divided by the sum of the mask coefficients, N , as shown in (4).

$$g(x, y) = \frac{1}{N} \times \sum_{s=-1}^1 \sum_{t=-1}^1 w(s, t) * f(x + s, y + t). \quad (4)$$

4.3 Band Pass Filter

Band pass filter is employed to accept frequencies within a range and to reject frequencies outside of that range. In this research, the filter bands are determined based on three factors: ASTM standard, the macrottexture definition, and the raw image resolution. Based on ASTM Standard, the band ranged from 10 to 400 cycle/m should be utilized to compute the MPD (ASTM E1845-15, 2015). The wave number of interest for PSD mainly concentrate between 20 and 500 cycle/m according to the macrottexture definition (20 to 2000 cycle/m) and the Nyquist sampling theorem (<500 cycle/m) (Hall et al., 2006; Sayers and Karamihas, 1996).

The Butterworth filter is used to eliminate the unwanted wavelengths, as defined in (5) (Gauch, 2010):

$$H(u, v) = \frac{1}{1 + \left[\frac{2(D(u, v) - D_H)}{D_H - D_L} \right]^{2n}} \quad (5)$$

Where $H(u, v)$ represents the response or gain; D_L is cut-off frequency for low pass filter; D_H is cut-off frequency for high pass filter; n is the order of Butterworth filter ($n=2$); $D(u, v)$ is the distance from a point (u, v) to the origin, as shown in (6).

$$D(u, v) = \left[\left(u - \frac{N}{2} \right)^2 + \left(v - \frac{M}{2} \right)^2 \right]^{1/2} \quad (6)$$

Where N and M represent the width and height of the image.

Fig. 4 shows the example of band pass filter to eliminate unwanted wavelengths. Note that wave numbers between f_1 and f_2 are unchanged. There is a gradual discontinuity between passed and rejected frequencies or wave number. However, the frequencies are completely suppressed for outside the band ranges in Fourier image.

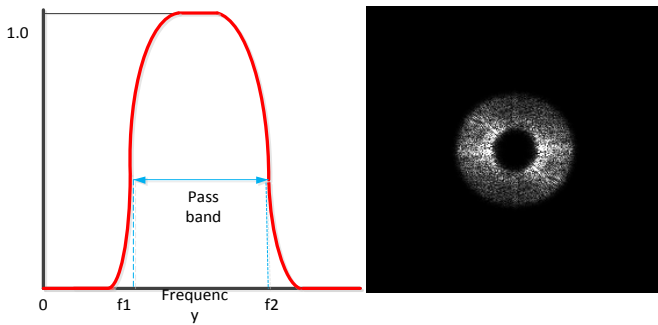


Fig. 4 Schematic for Butterworth band pass filter

4.4 Software Interface

To explore the impacts of sample size on the calculation of texture indicators, the user-friendly interface software was developed, as given in Fig. 5. Through opening the database file, the image quantity contained in the data collection is loaded into this software, and simultaneously the section length are recorded in meters or feet. Afterwards, the sample widths and lengths can be customized through the edit boxes embedded into the software, and the section beginning location and section length of concern can be trimmed by specifying the initial image ID and the number of samples that intends to be processed. Upon making all these parameters ready, the “Process” is clicked to calculate texture indicators of interest by checking the options in the check boxes. Once the processing is completed, the outputs can be displayed in the list control and exported into the specified storage device drives.

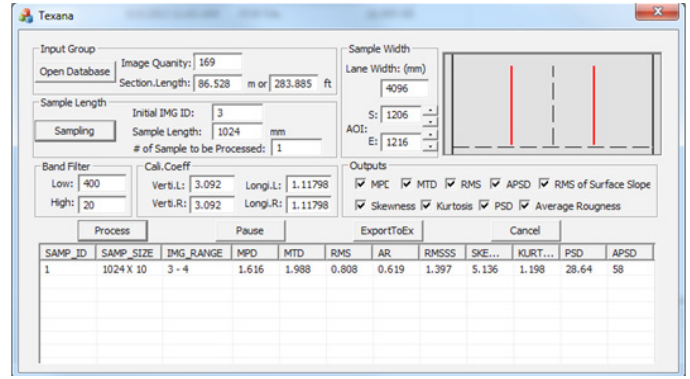


Fig. 5 Screenshots of software interface

5 Results and Analyses

After invalid data are repaired using neighbourhood averaging approach and unwanted wavelengths are filtered out with Butterworth band pass filter, various sample widths and lengths are investigated to study the impacts of sample size on the computation of texture indicators. For instance, MPD-Lm represents that MPD is calculated based on a sample with a length of m raw images, and the MPD-Wn represents MPD is calculated from a sample with a width of n millimeters. Similar name conventions are used for the MTD and PSD calculations.

To explore the impacts of sample lengths on MPD computation, five different sample lengths (MPD-L1, MPD-L2, MPD-L4, MPD-L8, and MPD-L16) with the same sample width (256) mm are tested. In this paper, MPD-L16 is selected as the reference sample, and the sample with a length less than 16 raw images is compared to the reference. Because the reference sample may cover several comparison samples in image quantity, the MPDs calculated from comparison samples should be transformed into the form that can be comparable with the reference sample, as shown in (7).

$$\text{Transformed } MPD_i(L16) = \frac{n}{16} \times \sum_{j=(i-1)*N+1}^{i*N} MPD_j(Ln) \quad (7)$$

Where i represents the i^{th} reference sample; j represents the j^{th} comparison sample; n is the number of raw images contained in the comparison sample ($n=1, 2, 4, \text{ or } 8$); N is the number of comparison samples within a reference sample (16 images).

For instance, assuming one data collection consists of 16 raw images, which includes one (16/16) reference sample, or 8 (16/2) comparison samples if a sample length of two raw images is used. The transformed MPD-L16 can be computed as the mean of the sum of the adjacent eight MPD-L2s, as shown in Fig. 6. The same approach is used for the computation of the transformed MTD-L16 and PSD-L16.

Similarly, to explore the impacts of sample widths on MPD computation, five different sample widths (MPD-W1, MPD-W4, MPD-W16, MPD-W64, and MPD-W256) with the same sample length (16 raw images) are investigated. MPD-W256 is selected as the reference sample, and the sample with a width less than 256mm is compared to the reference. These five

sample widths are also used to study the impacts of widths on the calculation of MTD and PSD.

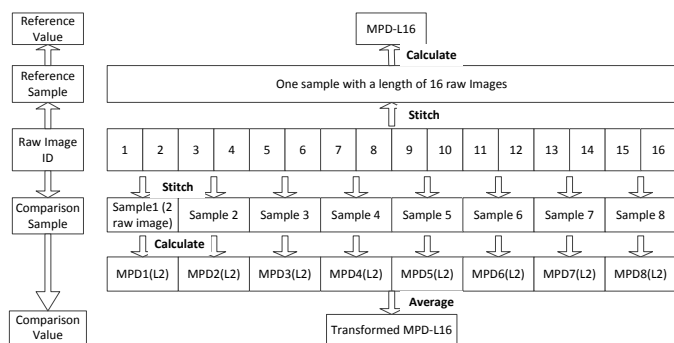


Fig. 6 Transformed MPD-L16 computation process

Two statistical methodologies are performed to study the impacts of sample size on the calculation of texture indicators. First, Analysis of Variance (ANOVA) test is used to investigate whether the calculated texture indicators using various sample size are statistically significantly different. If no significant differences are observed among the texture indicators calculated using various sample lengths or widths, it is concluded that sample lengths or widths has no impact on the calculation of the texture indicators. Second, if significant differences are observed, linear regression analysis is performed to examine whether the MPDs calculated from various sample lengths or widths are highly correlated with the reference.

5.1 Effects of Sample Size on MPD Calculation

ANOVA test results are shown in Table 3. P-value or F-value in the table indicates that the influences of sample lengths and widths on the MPD computation are statistically significant at 95% confidence level. In other words, MPDs calculated with various sample sizes (length and width) are not identical and the impact of sample size should be considered when computing MPD values.

Afterwards, linear regression analysis is employed to study the relationships among MPDs, as shown in Table 4. The test sites 5 to 7 are PCC pavements, while other four sites are AC pavements. It can be seen that the larger the sample width or length is used for MPD calculation, the higher the determinants of coefficients between comparison samples and the reference sample are for both AC and PCC pavements. However, the R-squared values are low and it is not adequate to develop robust regression models to correlate these MPDs at various sample lengths. For effects of sample width on MPD computation, the R-squared values range from 0.04 to 0.83 for AC pavement; the correlations among the MPDs for the PCC pavements are excellent for sample widths that exceed 4 mm, with R-squared ranging from 0.95 to 0.98. In other words, the MPD computation for AC pavements is more sensitive to the sample widths than that for PCC pavement.

Table 3 ANNOVA analysis: effect of sample size on MPD calculation

ANOVA Test		df	F	P-value	F crit
Site 1	Length	4	2.38E+03	3.44E-113	2.45E+00
	Width	3	1.30E+01	3.23E-07	2.70E+00
Site 2	Length	4	3.05E+02	7.19E-62	2.45E+00
	Width	3	4.25E-02	9.88E-01	2.70E+00
Site 3	Length	4	8.99E+02	5.32E-83	2.45E+00
	Width	3	2.66E+00	5.31E-02	2.70E+00
Site 4	Length	4	4.96E+02	1.32E-73	2.45E+00
	Width	3	4.08E+01	4.31E-17	2.70E+00
Site 5	Length	4	8.37E+02	5.48E-84	2.45E+00
	Width	3	8.77E+00	3.57E-05	2.70E+00
Site 6	Length	4	2.15E+03	1.39E-110	2.45E+00
	Width	3	2.33E+00	7.91E-02	2.70E+00
Site 7	Length	4	4.28E+02	5.53E-70	2.45E+00
	Width	3	2.33E+00	7.88E-02	2.70E+00

Table 4 Linear regression analysis: effects of sample size on MPD

Correlated Indicators	R-squared at Test Site						
	1	2	3	4	5	6	7
L16 / L1	0.00	0.41	0.57	0.20	0.22	0.50	0.64
L16 / L2	0.00	0.59	0.51	0.23	0.20	0.53	0.64
L16 / L4	0.15	0.79	0.63	0.21	0.24	0.55	0.68
L16 / L8	0.65	0.96	0.76	0.49	0.18	0.67	0.75
W256 / W1	0.00	0.10	0.05	0.02	0.16	0.13	0.17
W256 / W4	0.62	0.78	0.74	0.80	0.92	0.85	0.95
W256 / W16	0.66	0.82	0.85	0.71	0.97	0.91	0.97
W256 / W64	0.54	0.96	0.94	0.89	0.98	0.94	0.98

In summary, the effects of both sample lengths and widths on MPD computation should be considered. However, for PCC pavements, the impacts of sample width on MPD calculation could be ignored if the sample width exceeds 4 mm.

5.2 Effects of Sample Size on MTD Calculation

Table 5 shows that significant differences exist among MTDs calculated using various sample widths and lengths. Therefore, the influence of sample widths and lengths on the MTD calculation is negligible. In terms of the effects of sample lengths on MTD computation, a fair correlation exists among these MTDs for both AC and PCC pavements, with R-squared values ranging from 0.45 to 0.98, as described in Fig. 7(a).

Fig. 7(b) shows the influence of sample width on MTD computation. For AC pavements, no satisfactory regression models can be developed due to the high standard deviation and low correlations. For PCC pavements, although better correlations and lower standard deviation are obtained, the R-squared values are still not adequate to develop regression models to correlate these indicators. It can be concluded that the influence of sample width on MTD computation should be considered for both AC

and PCC pavements, especially for AC pavements since its MTD computation is more sensitive to the sample widths.

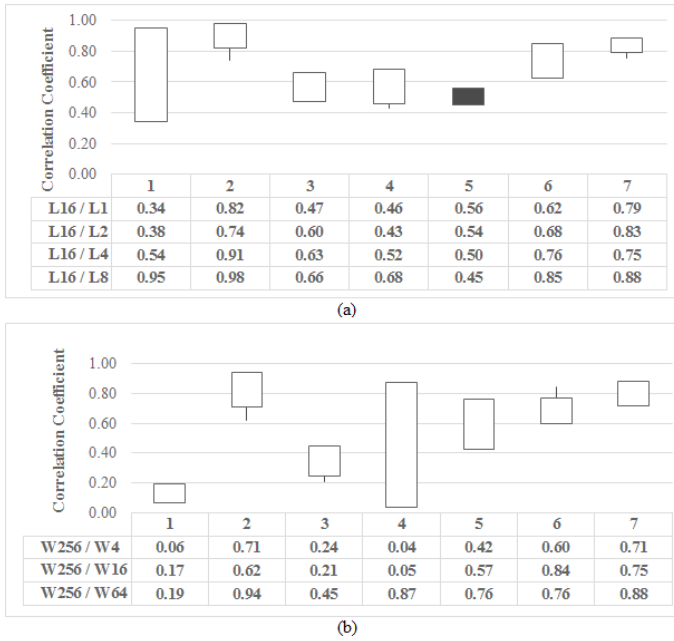


Fig. 7 Impacts of sample size on MTD calculation; a) Sample length; b) Sample width

Table 5 ANNOVA analysis: effect of sample size on MTD calculation

ANOVA Test		df	F	P-value	F crit
Site 1	Length	4	4.48E+02	4.02E-71	2.45E+00
	Width	3	5.76E+02	3.12E-61	2.70E+00
Site 2	Length	4	7.18E+01	6.34E-31	2.45E+00
	Width	3	2.48E+02	4.80E-45	2.70E+00
Site 3	Length	4	1.61E+02	3.02E-47	2.45E+00
	Width	3	1.91E+03	1.06E-82	2.70E+00
Site 4	Length	4	4.26E+02	7.07E-70	2.45E+00
	Width	3	2.30E+03	3.38E-89	2.70E+00
Site 5	Length	4	4.22E+02	1.06E-67	2.45E+00
	Width	3	9.93E+02	6.41E-70	2.70E+00
Site 6	Length	4	1.34E+03	1.83E-98	2.45E+00
	Width	3	1.84E+03	1.27E-84	2.70E+00
Site 7	Length	4	4.48E+02	4.02E-71	2.45E+00
	Width	3	1.99E+02	4.96E-41	2.70E+00

5.3 Effects of Sample Size on PSD Calculation

Table 6 shows that significant differences exist among PSDs calculated using various sample widths and lengths. Therefore, the influence of sample widths and lengths on the PSD calculation is not negligible.

For the impacts of sample lengths on PSD computation, it can be observed that the poor correlation exists for both AC and PCC pavements (Fig. 8a), that is, the attentions should be paid when the different sample lengths are used to calculate PSD. As for the effects of sample widths on PSD calculation, it can be observed that a fair correlation exists for AC pavements and a strong correlation exists for PCC pavements (Fig. 8b). In other

words, the effects of sample widths on PSD calculation for PCC pavements can be ignored if the sample widths exceed the 4 mm.

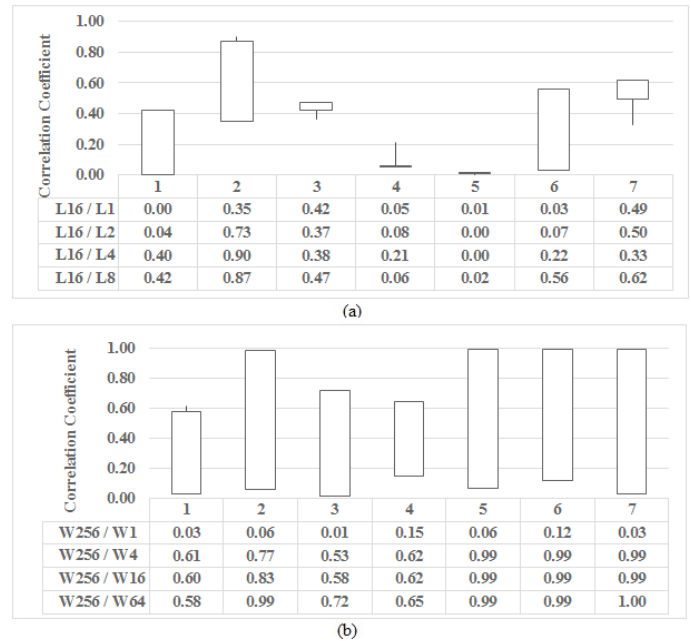


Fig. 8 Impacts of sample size on PSD calculation; a) Sample length; b) Sample width

Table 6 ANNOVA analysis: effect of sample size on MTD calculation

ANOVA Test		df	F	P-value	F crit
Site 1	Length	4	4.89E+02	3.05E-73	2.45E+00
	Width	3	2.63E+02	3.90E-46	2.70E+00
Site 2	Length	4	3.79E+02	4.69E-67	2.45E+00
	Width	3	6.82E+01	1.06E-23	2.70E+00
Site 3	Length	4	1.07E+03	9.18E-93	2.45E+00
	Width	3	2.33E+02	7.25E-43	2.70E+00
Site 4	Length	4	6.77E+02	2.61E-81	2.45E+00
	Width	3	3.54E+01	1.73E-15	2.70E+00
Site 5	Length	4	2.81E+02	2.54E-58	2.45E+00
	Width	3	4.95E+01	3.80E-19	2.70E+00
Site 6	Length	4	1.35E+03	1.23E-98	2.45E+00
	Width	3	2.63E+02	3.90E-46	2.70E+00
Site 7	Length	4	2.18E+02	4.97E-54	2.45E+00
	Width	3	7.10E+00	2.34E-04	2.70E+00

It should be noted that poor correlations are obtained between the reference texture indicators (e.g. MPD-W256, PSD-W256) and those calculated based on one single longitudinal profile (e.g. MPD-W1, PSD-W1), as shown on in Fig. 8b or Table 4. There are two potential reasons causing the differences. One reason is that different data repair mechanisms are applied. For one single longitudinal profile (profile-based) data, the invalid pixel value is replaced by averaging the previous and following pixel values along this profile. While the adjacent eight neighboring pixels of the invalid point are used to repair the invalid reading if the sample has a certain width (area-based).

The other reason is that different Fourier transform principles are applied. The profile based data can be regarded as one-dimensional signal, and one-dimensional Fourier transform is applied in the frequency domain. However, the area-based data are two-dimensional, and the Fourier transform is conducted not only in the traveling direction, but also in the direction perpendicular to traveling direction.

6 Conclusions

In this study the impacts of sample size on the computations of MPD, MTD, and PSD are explored using 1mm 3D surface texture data. After invalid data points are repaired and Butterworth filter is applied to remove unwanted wavelengths, ANNOVA test and linear regression analysis are performed. The findings indicate that the impacts of sample lengths on the computation of these three texture indicators are significant and attention should be paid when different sample lengths are used to calculate those indicators. As for the impacts of sample widths on the computation of texture indicators, the findings indicate that the impacts of sample widths on MTD computation should be considered for both AC and PCC pavements, while the effects of sample width on MPD and PSD calculations for PCC pavements can be ignored if sample width is wider than 4mm since good regression models can be developed between the reference and comparison MPDs or PSDs.

Current practices of computing texture indicators are based on line-of-sight technology. From this research, it is found that the indicators calculated from various sample size are significantly different from those obtained from a point laser data. Therefore, it is apparent that texture analysis and its standardization with 1mm 3D surface data are necessary as 3D data collection at true 1mm resolution with full coverage of pavement surface is becoming a reality. Current ASTM and other procedures cannot be directly applied to 3D surface for production due to a lack of definitions. With further research by investigating broader sample widths (e.g. 1024mm and 512mm) and comparing with field measured data, it is anticipated that efforts to determine reasonable pavement sample size through the application of 3D surface data will be made.

References

- Abbas, A., Kutay, M. E., Azari, H., Rasmussen, R. (2007). Three-Dimensional Surface Texture Characterization of Portland Cement Concrete Pavements. *Computer-Aided Civil and Infrastructure Engineering*. 22(3), pp. 197-209. <https://doi.org/10.1111/j.1467-8667.2007.00479.x>
- ASME. (2009). *Surface Texture (Surface Roughness, Waviness, and Lay)*. ASME B46.1, American Society of Mechanical Engineers, Three Park Avenue, New York, NY.
- ASTM E867-06 (2012). *Standard Terminology Relating to Vehicle-Pavement Systems*. ASTM International, West Conshohocken, PA. <https://doi.org/10.1520/E0867-06R12>
- ASTM E2157-15. (2015). *Standard Test Method for Measuring Pavement Macrotecture Properties Using the Circular Track Meter*. ASTM International, West Conshohocken, PA. <https://doi.org/10.1520/E2157-15>
- ASTM E1845-15. (2015). *Standard Practice for Calculating Pavement Macrotecture Mean Profile Depth*. ASTM International, West Conshohocken, PA. <https://doi.org/10.1520/E1845-15>
- ASTM E965-15. (2015). *Standard Test Method for Measuring Pavement Macrotecture Depth Using a Volumetric Technique*. ASTM International, West Conshohocken, PA. <https://doi.org/10.1520/E0965-15>
- El Gendy, A., Shalaby, A. (2007). Mean profile depth of pavement surface macrotecture using photometric stereo techniques. *Journal of Transportation Engineering*. 133(7), pp. 433-440. [https://doi.org/10.1061/\(ASCE\)0733-947X\(2007\)133:7\(433\)](https://doi.org/10.1061/(ASCE)0733-947X(2007)133:7(433))
- Ergun, M. D., Agar, A. (2000). Optimization of Road Surface Friction from Macro and Micro Texture Point of View. In: SURF 2000: Fourth International Symposium on Pavement Surface Characteristics on Roads and Airfields, Nantes, France, 22-24 May 2000, pp. 217-226.
- Flintsch, G. W., de León, E., McGhee, K., Al-Qadi I. L. (2003). Pavement Surface Macrotecture Measurement Applications. *Transportation Research Record: Journal of the Transportation Research Board*. 1860, pp. 168-177. <https://doi.org/10.3141/1860-19>
- Gauch, J. (2010). Digital Image Processing. Computer Science, University of Arkansas, Arkansas. [Online]. Available from: <http://csce.uark.edu/~jgauch/5683/notes/ch04c.pdf>. [Accessed: 8th January 2015]
- Hall Jr, J. W., Smith, K. L., Titus-Glover, L., Wambold, J. C., Yager, T. J., Rado, Z. (2009). Guide for Pavement Friction. Final Report for NCHRP Project 01-43. National Cooperative Highway Research Program (NCHRP). Transportation Research Board of the National Academies, Washington, D.C. <https://doi.org/10.17226/23038>
- International Standards Organization (ISO). (1997). *Characterization of Pavement Texture using Surface Profiles – Part 1: Determination of Mean Profile Depth*. ISO Standard 13473-1:1970. International Standards Organization, Geneva, Switzerland.
- Li, L., Wang, K. C., Li, Q. J. (2016). Geometric texture indicators for safety on AC pavements with 1mm 3D laser texture data. *International Journal of Pavement Research and Technology*. 9(1), pp. 49-62. <https://doi.org/10.1016/j.ijprt.2016.01.004>
- Luo, W., Wang, K. C. P., Li, L. (2015). Hydroplaning on Sloping Pavements Based on Inertial Measurement Unit (IMU) and 1mm 3D Laser Imaging Data. *Periodica Polytechnica Transportation Engineering*. 44(1), pp. 42-49. <https://doi.org/10.3311/PPtr.8208>
- Luo, W., Wang, K., Li, L., Li, Q., Moravec, M. (2014). Surface Drainage Evaluation for Rigid Pavements Using an Inertial Measurement Unit and 1-mm Three-Dimensional Texture Data. *Transportation Research Record: Journal of the Transportation Research Board*. 2457, pp. 121-128. <https://doi.org/10.3141/2457-13>
- Meegoda, J. N., Gao, S. (2015). Evaluation of pavement skid resistance using high speed texture measurement. *Journal of Traffic and Transportation Engineering (English Edition)*. 2(6), pp. 382-390. <https://doi.org/10.1016/j.jtte.2015.09.001>
- Sengoz, B., Topal, A., Tanyel, S. (2012). Comparison of pavement surface texture determination by sand patch test and 3D laser scanning. *Periodica Polytechnica Civil Engineering*. 56(1), pp. 73-78, 2012. <https://doi.org/10.3311/pp.ci.2012-1.08>

- Torbruegge, S., Wies, B. (2015). Characterization of pavement texture by means of height difference correlation and relation to wet skid resistance. *Journal of Traffic and Transportation Engineering (English Edition)*. 2(2), pp. 59-67.
<https://doi.org/10.1016/j.jtte.2015.02.001>
- Sayers, M. W., Karamihas, S. M. (1996). Interpretation of road roughness profile data. Contract DTFH 61-92-C00143. Federal Highway Administration.
<http://citeseerx.ist.psu.edu/viewdoc/download?doi=10.1.1.40.5876&rep=rep1&type=pdf>
- Wang, K. C., Hou, Z., Gong, W. (2008). Automation Techniques for Digital Highway Data Vehicle (DHDV). In: Seventh International Conference on Managing Pavement Assets. URL: <http://citeseerx.ist.psu.edu/viewdoc/download?doi=10.1.1.651.9565&rep=rep1&type=pdf>
- Wang, K. C., Li, L., Luo, W., Larkin, A. (2012). Potential Measurement of Pavement Surface Texture Based on Three-Dimensional Image Data. In: *Transportation Research Board 91st Annual Meeting*. Washington, DC., USA, Jan. 22-26, 2012. p. 17.